Applied Thermal Engineering 149 (2019) 1492–1502

Contents lists available at ScienceDirect

Applied Thermal Engineering

journal homepage: www.elsevier.com/locate/apthermeng

Research Paper

The impact of heat exchanger degradation on the performance of a humid air turbine system for power generation

Pau Lluis Orts-Gonzalez, Pavlos K. Zachos*, Giovanni D. Brighenti

Propulsion Engineering Centre, School of Aerospace, Transport and Manufacturing, Cranfield University, Cranfield MK43 0AL, Bedfordshire, United Kingdom

HIGHLIGHTS

- Effect of the air-water heat exchanger's degradation on the performance of the reheated humid air turbine is evaluated.
- Cycle irreversibilities associated with heat exchanger degradation are identified via exergy analysis.
- The highest penalties on efficiency and power output are associated with the intercooler's deterioration.
- The intercooler's degradation has a first order impact on the operability range of the low pressure compression system.
- Performance penalties can be partially mitigated by introducing more effective heat exchangers at a higher acquisition cost.

ARTICLE INFO

Keywords:
Humid air turbine
Evaporative gas turbine
Heat exchanger
Degradation analysis
Exergy analysis

ABSTRACT

This paper aims to analyse the impact of air-water heat exchanger's degradation on the performance of a reheated humid air turbine system for power generation applications. A number of thermal models to simulate the performance of the various sub-systems was put together and validated against experimental data. The performance degradation of the heat exchangers is characterised by means of a degradation coefficient, which is used to drive the cycle into off-design and part-load conditions when degradation is accounted for. Three heat exchanger design scenarioswere investigated, namely a low, a medium and a high effectiveness in order for the impact of the degradation penalties on cycle thermal efficiency to be determined. The performance deterioration of the heat exchangers is also analysed from an exergetic point of view in order to identify the key sources that penalise the thermal efficiency of the humid air turbine system. The degradation analysis shows that typical levels of intercooler deterioration cause notable penalties in the cycle performance, reducing its thermal efficiency and power output by 1.8 percentage points and 28% respectively compared to the un-degraded operation. The exergy analysis showed that the deterioration of the intercooler also penalises the efficiency of the low pressure compressor and reheater, which contribute to the performance penalty of the cycle too. It is also found that the degradation of the intercooler can also lead to operability penalties at the low pressure compressor by reducing its surge margin. The effects of the deterioration of the aftercooler and economiser were found to only have a weak effect on the system's performance. The outcome of the work constitutes a step forward in understanding of the performance behaviour of an advanced cycle when heat exchanger degradation is present.

1. Introduction

Over the past decades, the development of new technologies in the power generation sector was focused on the enhancement of thermal efficiency together with reduction of emission levels. Among various possible approaches to address these challenges, Humid Air Turbines (HAT), also called Evaporative Gas Turbines (EvGT), were introduced as a promising concept by Jonsson and Yan [1] and Yagi et al. [2]. Since the early introduction of HAT systems in the late 80's by Rao [3], numerous studies showed the highly efficient variations of such cycles and their advantageous economic performance. Lazzaretto and Segato [4,5] introduced a high efficiency configuration using an intercooler, aftercooler, and economiser to recuperate a notable amount of heat back into the cycle. Ågren and Westermark [6,7] suggested that a percentage of the inlet mass flow should bypass the aftercooler and saturator to further improve cycle performance. Chiesa et al. [8] showed that the addition of a second combustion chamber could improve the thermal efficiency beyond the 60% thershold, which was also

* Corresponding author.
E-mail address: p.zachos@cranfield.ac.uk (P.K. Zachos).

https://doi.org/10.1016/j.applthermaleng.2018.12.061
Received 20 March 2018; Received in revised form 28 October 2018; Accepted 12 December 2018
Available online 13 December 2018
1359-4311/

Nomenclature

Symbols

ΔP	pressure loss, Pa
ΔP_f	pressure drop penalty coefficient, –
A_{HE}	heat transfer area, m^2
C	carbon atomic fraction, –
DC	degradation coefficient, –
$\dot{E}x$	exergy, W
f	friction factor, –
$\dot{G}$	mass flux, kg/s m^2
H	hydrogen atomic fraction, –
h	specific enthalpy, J/kg
k_{film}	thermal conductivity of the fouling film, W/m K
L_{flow}	length of the flow passage, m
LHV	low heating value, J/kg
$\dot{m}$	mass flow, kg/s
P	pressure, Pa
$\dot{Q}$	heat transferred, W
R_f	fouling resistance, m^2 K/W
s	specific entropy, J/kg K
T	temperature, K
t_{film}	thickness of the fouling film, m
U	overall heat transfer coefficient, W/m^2 K
$\dot{W}$	power, W

Abbreviations

AC	Aftercooler
AWHE	Air-Water Heat Exchanger
CC	Combustion Chamber
CCGT	Combined Cycle Gas Turbine
EC	Economiser
EvGT	Evaporative Gas Turbine
FPT	Free Power Turbine
HAT	Humid Air Turbine
HPC	High Pressure Compressor
HPT	High Pressure Turbine
IC	Intercooler
LPC	Low Pressure Compressor
LPT	Low Pressure Turbine
M_{FPT}	Mixer of Free Pressure Turbine cooling flows
M_{HPT}	Mixer of High Pressure Turbine cooling flows
M_{LPT}	Mixer of Low Pressure Turbine cooling flows
M_{SAT}	Mixer of Saturator bypass duct
NTU	Number of Transfer Units
OUT	Exhaust
pp	percentage point
RC	Recuperator
RH	Reheater
RHAT	Reheated Humid Air Turbine
SAT	Saturator
Sim	Simultaneous

Subscripts

a	dry air or airside
c	cold flow
clean	clean conditions
comp	compressor
deg	degraded conditions
dest	destroyed
DP	design point
f	fouled conditions
fuel	fuel
g	gas/humid air
h	hot flow
HE	Heat Exchanger
in	inlet
o	reference conditions
out	outlet
Ref	design point conditions
tot	overall
turb	turbine
v	water vapour
w	water or waterside

Greek symbols

α	coefficient, –
β	heat transfer coefficient, W/m^2 K
ε	effectiveness, –
ρ	density, kg/m^3
ψ	specific flow exergy, W/kg
ω	water to air ratio, –

later confirmed by Nakhamkin et al. [9] and Brighenti et al. [10] .

Further economic studies also demonstrated the potential benefits of HAT systems. Jonsson and Yan [11] compared the techno-economic performance of a HAT cycle against a Combined Cycle Gas Turbine (CCGT) showing that for a similar cost of the electricity, the HAT cycle offers a 12–15% lower specific investment cost. Further studies, such as the ones presented by Kavanagh and Parks [12,13] and Traverso and Masardo [14] showed that a HAT system is capable of achieving up to 7% lower cost of the electricity than a CCGT. In terms of part load performance, Takahashi et al. [15] demonstrated that the part load efficiency penalty of a HAT system is up to a 10% lower compared to a typical CCGT across a similar range of operating conditions. Finally, Wang et al. [16] and Kim et al. [17] proved that the performance of the HAT was also less affected by the change in ambient conditions compared to a typical CCGT.

On the downside, the potential efficiency and cost benefits of a HAT or a CCGT system heavily rely on a number of heat exchanger units as part of the cycle. These heat exchangers are susceptible to fouling which may cause notable penalties on their effectiveness and have a detrimental effect on the thermal performance of the whole system [18–21]. More specifically, various types of deposits on the inner walls of the heat exchangers can reduce its heat transfer coefficient with notable effects on the overall effectiveness of the unit. Some of these effects were previously quantified for a combined steam-gas system by Zwebek and Pilidis [22,23] who concluded that a 5% deterioration of the heat exchangers of a CCGT may cause up to 1.5% reduction in work and efficiency.

Nevertheless, no previous research has quantified the impact of heat exchanger deterioration to the cycle performance for a HAT system which is the topic of the present work. In this paper the performance degradation effects of a number of heat exchangers on the thermal output and economic performance of a 40 MW advanced HAT system are determined. A new approach to simulate the degraded performance of the heat exchangers and the integration into the whole cycle off-design model was developed. The effect of the air-water heat exchanger's degradation on the system's performance is shown for three design scenarios across a range of heat exchanger's technology levels. Finally, exergy analysis was used to identify the key system components

affected by the variations of the heat exchanger's effectiveness due to the degradation effects.

2. Methodology

2.1. Cycle configuration

The Reheated Humid Air Turbine (RHAT) analysed herein(Fig. 1) was previously presented by Brighenti et al. in [10]. The heat exchanger configuration is selected to maximise the heat recuperated within the cycle, as suggested by Nyberg and Thern [24]. A saturator bypass duct is included to enhance the thermal efficiency, as recommended by Ågren and Westermark [6,7]. The reheater is added in order to further augment the thermal efficiency and specific power, as recommended by Chiesa et al. [8] and demonstrated by Brighenti et al. [10]. An open loop is used to feed water in the heat exchangers as discussed by Rosen [25]. The intercooler and the aftercooler are assumed to be plate-fin heat exchangers, whereas the economiser is considered as a tube-fin heat exchanger as previously presented by Brighenti et al. [10]

The cycle definition at design point is presented in Table 1. The selected values are reasonable assumptions based on current gas turbine and heat exchanger technology levels [11,12,14,26,27].

The effectiveness of all air-water heat exchangers represents the "technology level" of the units and is considered to be variable as an indicator of heat exchanger degradation levels. Three heat exchanger design scenarios in terms of effectiveness were analysed as part of the present study and are presented in Table 2.

The performance of the air-water heat exchangers is parametrically degraded by increasing the fouling resistance on the airside and waterside respectively ($R_{f,a}$ and $R_{f,w}$), and the pressure drop coefficient (ΔP_f). The level of deterioration is characterised by the Degradation Coefficient (DC) defined in Eq.(1). The fouling resistance of both sides and the pressure drop penalty coefficient are normalised against the reference values [20,28–30] shown in Table 3. For the current analysis, the imposed DC ranges from 0 to 2.0 which drives the cycle to off-design, while the turbine inlet temperature of 1600 K was kept constant across both combustors.

$$DC \equiv \frac{R_{f,a}}{(R_{f,a})_{Ref}} = \frac{R_{f,w}}{(R_{f,w})_{Ref}} = \frac{\Delta P_f}{(\Delta P_f)_{Ref}} \quad (1)$$

Table 1
Cycle design point definition.

Nominal power output	40 MW
Combustor and reheater turbine inlet temperature	1600 K
Overall compressor pressure ratio	40
Recuperator effectiveness	0.90
Compressor polytropic efficiency	0.90
Core turbine polytropic efficiency	0.90
Power turbine polytropic efficiency	0.92
Combustion chamber efficiency	0.999
Combustion chamber pressure loss	5%
Saturator pinch point	5 K
Saturator pressure loss	5%
Air-water heat exchangers airside pressure loss	7.5%
Cold-side recuperator pressure loss	7.5%
Hot-side recuperator pressure loss	5%
Maximum allowed blade metal temperature	1300 K
Film cooling effectiveness	0.40
Internal flow cooling efficiency	0.70
Inlet air pressure	1 atm
Inlet air temperature	288.15 K
Inlet air relative humidity	80%

Table 2
Air-water heat exchanger's effectiveness envelopes analysed.

Cycle design variable	Design scenario		
	Low	Average	High
Intercooler, aftercooler, economiser effectiveness	0.75	0.85	0.95

2.2. Cycle modelling

The numerical scheme to predict the part load performance of the RHAT system is based on the work previously shown by Brighenti et al. in [31]. The prediction platform relies on a number of component models to estimate their thermal behaviour across a range of operating conditions. The performance simulation platform and the workflow are shown in Fig. 2. The performance of the gas turbine and recuperator are resolved by TURBOMATCH [32,33] interfaced with MATLAB functions for the heat exchanger modelling. For the humidifier modelling, a new approach based on the Aramayo-Prudencio et al. [34] and Lindquist et al. [35] models has been developed as part of this work. This model was previously presented by Brighenti et al. [10,31] and validated against experimental data from Lindquist et al. [35]. A Broyden based

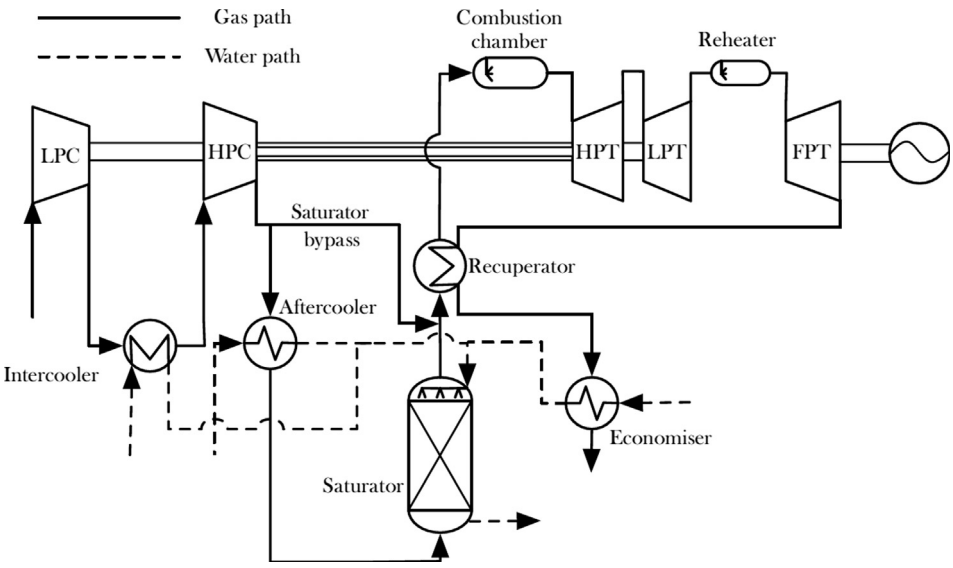

Fig. 1. Reheated humid air turbine system cycle layout [10].

Table 3
Reference fouling values.

	Side	R_f [m² K/kW]	ΔP_f
Intercooler, Aftercooler	Water	0.200 [28]	Calculated based on fouling film thickness
(plate-fin)	Air	0.176 [20]	32% [30]
Economiser	Water	0.200 [28]	Calculated based on fouling film thickness
(tube-fin)	Air	0.176 [20]	20% [29]

solver was used to match the system's components at part load [36]. The inputs were the thermodynamic design vector of the cycle, the ambient conditions, and the degradation coefficient imposed on the heat exchangers, which was the parameter driving the cycle to off-design.

The degradation of the heat exchangers is simulated using the fouling resistance ($R_{f,tot}$) as defined in Eq. (2), previously suggested by Kakaç and Pramuanjaroenkij [18]. $R_{f,tot}$ acts as a resistance that reduces the design overall heat transfer coefficient of the unit.

$$\frac{1}{(UA_{HE})_f} = \frac{1}{(UA_{HE})_{clean}} + R_{f,tot} \tag{2}$$

$(UA_{HE})_{clean}$ represents the product of the overall heat transfer coefficient at clean conditions and the heat transfer area, and $(UA_{HE})_f$ represents the same product at degraded conditions.

$R_{f,tot}$ is calculated as the weighted average of the fouling resistance of the airside and the waterside. This depends on the imposed degradation coefficient (DC) where the heat transfer areas (A_{HE}) of the airside and the waterside are used as weighting coefficients in Eq. (3), according to Kakaç and Pramuanjaroenkij [18].

$$\frac{R_{f,tot}}{A_{HE,tot}} = \frac{R_{f,a}\{DC\}}{A_{HE,a}} + \frac{R_{f,w}\{DC\}}{A_{HE,w}} \tag{3}$$

The off-design performance simulation of the heat exchangers also relies on the variation of the effectiveness produced by the change in the heat transfer coefficient. Assuming that the flow properties of both streams do not vary significantly compared to design point, the Prandtl number and the thermal conductivity of the fluid are considered to be constant. Hence, the variation of the heat transfer coefficient (β) is only a consequence of the variations in mass flow, Prandtl and Reynolds numbers (see Eq. (4)).

$$\beta \propto Nu \propto Re^n Pr^m \tag{4}$$

This assumption enables the scaling of the heat transfer coefficient at off-design conditions as in Eq. (5). $\dot{m}_w$ and $\dot{m}_g$ indicate the mass flows of the waterside and the airside respectively, the subscript *Ref* refers to the design point conditions and f to off-design condition of the heat exchanger due to fouling. For the water passages, the Dittus-Boelter heat transfer correlation was used to approximate the heat transfer coefficient, with a value of n_w of 0.8. For the plate-fin configurations, the airside heat transfer coefficient is also modelled by the Dittus-Boelter equation, which yields an n_g value of 0.8. For the airside heat transfer coefficient estimation at the tube-fin configurations, the ESDU approach shown in [37] was used, which yields an n_g value of 0.658.

$$(UA_{HE})_{off-design} = (UA_{HE})_{Ref}\left(\frac{\dot{m}_{w,f}^{n_w}\dot{m}_{g,f}^{n_g}}{\dot{m}_{w,Ref}^{n_w}\dot{m}_{g,Ref}^{n}}\right)\left(\frac{\dot{m}_{w,Ref}^{n_w} + \dot{m}_{g,Ref}^{n_g}}{\dot{m}_{w,f}^{n_w} + \dot{m}_{g,f}^{n_g}}\right) \tag{5}$$

Combining Eq. (2) and Eq. (5), the off-design performance of the heat exchangers represented by their $(UA_{HE})_f$ term was calculated as shown in Eq. (6). Once the $(UA_{HE})_f$ was known, the off-design effectiveness was calculated using the ε–NTU method proposed by Kays and London [38]. Thereafter, the outlet temperatures for the two streams

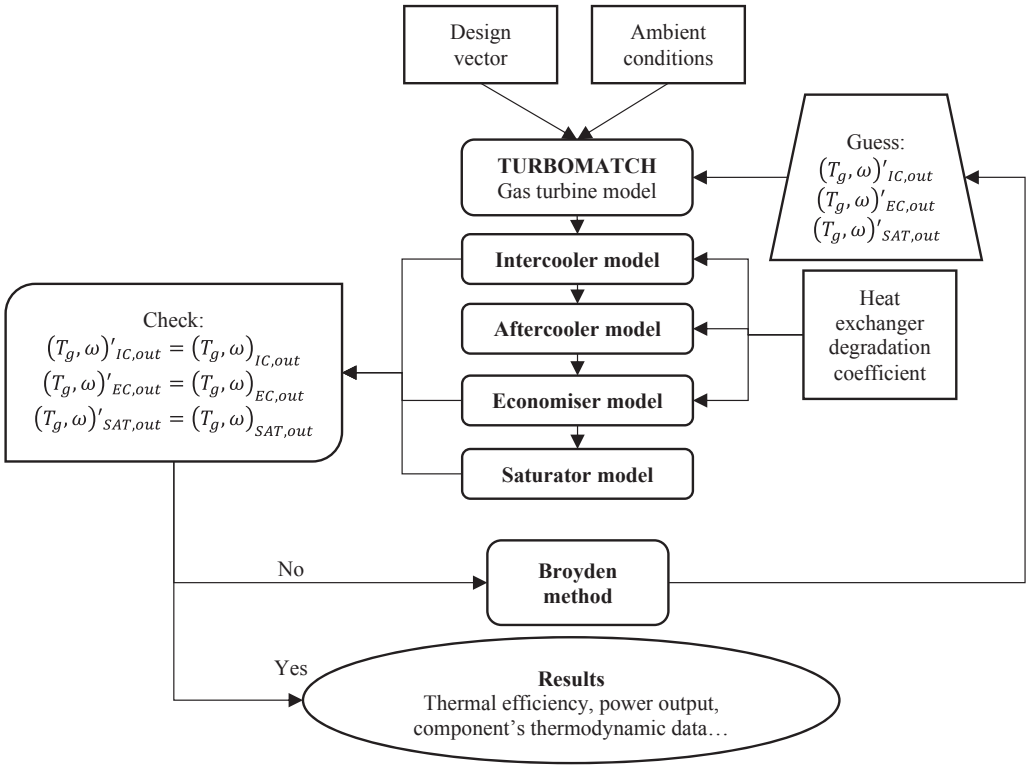

Fig. 2. Reheated humid air turbine off-design model flowchart.

were derived.

$$(UA_{HE})_f = \frac{1}{1/(UA_{HE})_{Ref} + R_{f,tot}} \left(\frac{\dot{m}_{w,f}^{nw} \dot{m}_{g,f}^{ng}}{\dot{m}_{w,Ref}^{nw} \dot{m}_{g,Ref}^{n}} \right) \left(\frac{\dot{m}_{w,Ref}^{nw} + \dot{m}_{g,Ref}^{ng}}{\dot{m}_{w,f}^{nw} + \dot{m}_{g,f}^{ng}} \right) \quad (6)$$

The airside pressure loss was estimated by means of a pressure loss coefficient as previously suggested by Walsh and Fletcher [39].

$$\frac{\Delta P}{P_{in}} = \alpha \left(\frac{\dot{m}_{in}\sqrt{T_{in}}}{P_{in}} \right)^2 \Delta P_f\{DC\} \quad (7)$$

Where α is a coefficient, whose value is calculated at design point, $\dot{m}_{in}$, T_{in} and P_{in} are the inlet mass flow, temperature and pressure respectively, and $\Delta P_f\{DC\}$ is a coefficient that accounts for fouling penalties ($\Delta P_f \geq 1$) and depends on the imposed degradation coefficient, DC.

The waterside pressure loss was calculated using Eq. (8), as previously presented by Kays and London [38]. L_{flow} represents the length of the flow passage and ρ the density of the fluid. The friction factor (f) was calculated as shown in the ESDU data items [40]. The water mass flux ($\dot{G}$) was defined as the mass flow per cross sectional flow area. The degraded hydraulic diameter (D_h) of the heat exchanger was calculated considering the thickness of the fouling film (t_{film}) and the hydraulic diameter at clean conditions ($D_{h|clean}$) as shown in Eq. (9).

$$\Delta P = \frac{4fL_{flow}\dot{G}^2}{2\rho D_h} \quad (8)$$

$$D_h = D_{h|clean} - 2t_{film} \quad (9)$$

The thickness of the film is estimated using the film's thermal conductivity (k_{film}) and $R_{f,w}$, which depends on the imposed deterioration coefficient, DC, as shown in Eq. (10) (see Ezgi et al. [41]). As the biofilm mass comprises mainly water (90–99%), the film's thermal conductivity, k_{film} is assumed to be equal to that of the water [41].

$$t_{film} = R_{f,w}\{DC\}k_{film} \quad (10)$$

2.3. Exergy analysis

Exergy analysis was previously applied on simple cycle gas turbines and humid air turbines [42–44] at design point and part-load operating conditions [45,46] to identify inefficiency sources within the system. For this study, an exergy analysis is further extended to include the effect of heat exchanger degradation on the cycle's performance.

The exergy destruction within a component is estimated by Eq. (11) (see Çengel and Boles [47]). A reference temperature of 288.15 K is assumed while reference partial pressures were evaluated at 1 atm and a relative humidity of 80%. The key assumptions made include steady flow, adiabatic components, no changes in kinetic or potential exergy, and ideal mixture of gases. It was previously found that an ideal gas mixture at high pressures yields an under-estimation of the humidity levels achieved at the exit of the saturator [48], which causes an under-prediction of the system's power output. However, as shown by Dalili et al. [48] no notable penalty in the thermal efficiency of the system is caused in such a case.

$$\sum \left(1 - \frac{T_o}{T_k}\right)\dot{Q}_k - \dot{W} + \sum (\dot{m}\psi)_{in} - \sum (\dot{m}\psi)_{out} = \dot{E}x_{dest} \quad (11)$$

$\dot{Q}_k$ represents the heat transferred to the system at temperature T_k, while T_o is the reference temperature, $\dot{W}$ is the output work delivered by the

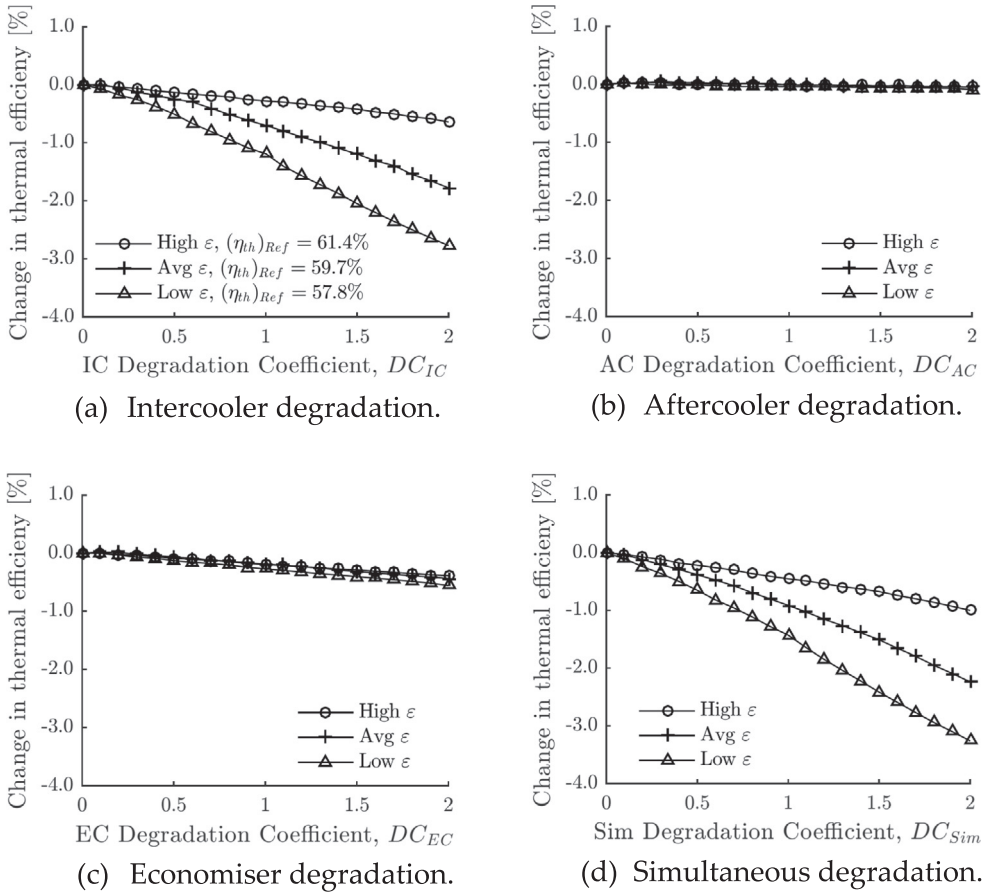

Fig. 3. Effect of the heat exchanger degradation level on cycle's thermal efficiency shown as departure from baseline efficiency calculated at clean (no degradation) conditions. (a) Intercooler degradation, (b) Aftercooler degradation, (c) Economiser degradation and (d) simultaneous degradation of heat exchanger units.

system, and $\dot{E}x_{dest}$ is the destroyed exergy within each component.

Gas and water specific flow exergy, ψ_g and ψ_w , are defined in Eqs. (12) and (13) for the gas and the water respectively (see Çengel and Boles [47]). h represents the specific enthalpy, s the specific entropy, and ω the water to air ratio of the gas defined as the quantity of water vapour divided by the quantity of dry air ($\dot{m}_v/\dot{m}_a$). Subscript zero indicates properties at the reference conditions, subscript g refers to the humid air, subscript a refers to the dry air, and subscript w refers to the water. Partial pressures were considered for the flow exergy calculations.

$$\psi_g = [(h - h_o) - T_o(s - s_o)]_a + \omega[(h - h_o) - T_o(s - s_o)]_w \tag{12}$$

$$\psi_w = [(h - h_o) - T_o(s - s_o)]_w \tag{13}$$

The consumed (or destroyed) exergy within each component as well as the rejected exergy was normalised by the exergy of the intriduced fuel, see Eq. (14).

$$\widehat{\dot{E}x_{dest,i}} = \frac{\dot{E}x_{dest,i}}{\dot{E}x_{in,fuel}} \tag{14}$$

Under the previous assumptions, the exergy balance of the cycle was determined using the following equations, derived from Eq. (11), for all system components.

Compressors:

$$\dot{E}x_{dest,comp} = \dot{W}_{comp} + (\dot{m}_g\psi_g)_{in} - (\dot{m}_g\psi_g)_{out} \tag{15}$$

Combustors:

$$\dot{E}x_{dest,CC} = (\dot{m}_{fuel}\psi_{fuel})_{in} + (\dot{m}_g\psi_g)_{in} - (\dot{m}_g\psi_g)_{out} \tag{16}$$

$$\psi_{fuel} = LHV\left(1.033 + 0.0169\frac{H}{C} - 0.0698\frac{1}{C}\right) \tag{17}$$

For the fuel exergy estimation in Eq. (16) only the chemical part is accounted for. In this study, the power plant was assumed to run with diesel oil, whose chemical composition is $C_{12}H_{23}$ (see Date [49]). LHV represents the low heating value of the fuel, H the hydrogen atomic fraction and C the carbon atomic fraction.

Turbines:

$$\dot{E}x_{dest,turb} = -\dot{W}_{turb} + (\dot{m}_g\psi_g)_{in} - (\dot{m}_g\psi_g)_{out} \tag{18}$$

Recuperator:

$$\dot{E}x_{dest,RC} = (\dot{m}_g\psi_g)_{h,in} + (\dot{m}_g\psi_g)_{c,in} - (\dot{m}_g\psi_g)_{h,out} - (\dot{m}_g\psi_g)_{c,out} \tag{19}$$

Air-water heat exchangers:

$$\dot{E}x_{dest,AWHE} = (\dot{m}_g\psi_g)_{in} + (\dot{m}_w\psi_w)_{in} - (\dot{m}_g\psi_g)_{out} - (\dot{m}_w\psi_w)_{out} - (\dot{m}_{cond}\psi_w)_{out} \tag{20}$$

The term $(\dot{m}_{cond}\psi_w)_{out}$ was added in Eq. (18) to account for the exergy of the possible water condensed from the moist in the air during the cooling process.

Saturator:

$$\dot{E}x_{dest,SAT} = (\dot{m}_g\psi_g)_{in} + (\dot{m}_w\psi_w)_{in} - (\dot{m}_g\psi_g)_{out} - (\dot{m}_w\psi_w)_{out} \tag{21}$$

Exhaust:

The rejected exergy was defined as the sum of the exergy of the gas flow at the exit of the economiser and the water flow exiting the saturator, as in Eq. (22):

$$\dot{E}x_{dest,OUT} = (\dot{m}_g\psi_g)_{EC,out} + (\dot{m}_w\psi_w)_{SAT,out} \tag{22}$$

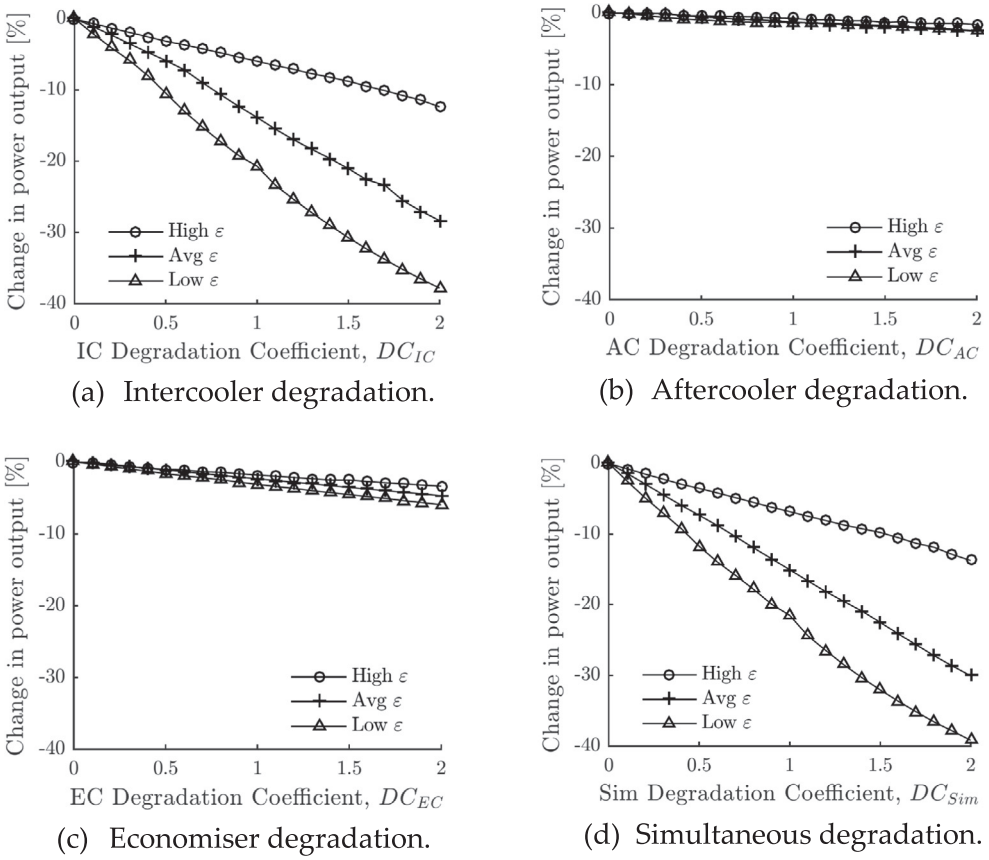

(a) Intercooler degradation. (b) Aftercooler degradation.

(c) Economiser degradation. (d) Simultaneous degradation.

Fig. 4. Effect of the heat exchanger degradation on the power output of the HAT system shown as departure from baseline power output calculated at clean conditions. (a) Intercooler degradation, (b) Aftercooler degradation, (c) Economiser degradation and (d) simultaneous degradation of all heat exchanger units.

3. Results and discussion

The effect of the air-water heat exchanger degradation on the thermal efficiency of the system is shown in Fig. 3. The intercooler deterioration was found to have the most notable impact on the thermal efficiency (Fig. 3a). For the average effectiveness design scenario, ε_{IC} = 0.85, and for DC_{IC} = 1, the thermal efficiency drops by 0.7 pp. This reduction becomes 1.8 pp for DC_{IC} = 2. The aftercooler degradation was found to also have a minor effect on the cycle's thermal efficiency (Fig. 3b). The degradation of the economiser has a less detrimental effect (Fig. 3c) as for the average baseline economiser effectiveness design scenario, the drop in the thermal efficiency forDC_{EC} = 2 is less than 0.5 pp. For simultaneous degradation of all three air-water heat exchanger units of the RHAT system, i.e. intercooler, economiser and aftercooler (see Fig. 3d), the thermal efficiency variation is the result of the combined penalties imposed by each heat exchanger. For the average heat exchanger effectiveness design and DC_{Sim} = 1 the thermal efficiency drops by 1.9 pp while for DC_{Sim} = 2 a 3 pp drop of thermal efficiency was found in comparison to clean operation.

As the baseline design effectiveness of the intercooler increases reaching the current state-of-the-art levels, the imposed penalties on the cycle's thermal efficiency become less notable. When the baseline design effectiveness of the intercooler becomes 0.95 from 0.85 (see Fig. 3a), only a 0.3 pp penalty in thermal efficiency is observed for DC_{IC} = 2. The aftercooler and economiser baseline effectiveness were found to have no notable impact on thermal efficiency (see Fig. 3b and c). Fig. 4 shows the power output penalties across a range of heat exchanger degradation coefficients. As anticipated, the degradation of the intercooler (Fig. 4a) causes the most notable penalties in power output. For the average intercooler effectiveness design scenario, ε_{IC} = 0.85, and DC_{IC} = 1, a 14% reduction in power output was observed in relation to the clean configuration while a 28% reduction was found for DC_{IC} = 2. The degradation level of the aftercooler or the economiser were found to have weaker impact. For the average aftercooler effectiveness design scenario, ε_{AC} = 0.85 and DC_{AC} = 1, a 1% penalty on power output (Fig. 4b) was found, whileDC_{EC} = 1 causes a roughly 2% reduction in the power output (Fig. 4c). When the degradation occurs in all three heat exchangers simultaneously, the overall power output was penalised by about 15% $DC_{Sim}$for = 1, and by 30% when DC_{Sim} = 2. Similarly to the efficiency variations, the highest rate of change in power output was found to occur for the low heat exchanger effectiveness design. As the design effectiveness increases, the effect of degradation on the reduction rate of the system's power output becomes less notable.

The impact of heat exchanger degradation on the exergy destroyed within each component is shown in Fig. 5 across a range of degradation rates for the average heat exchanger effectiveness design scenario as defined in Table 2. The lines connect the change in $\widehat{\dot{E}x_{dest}}$ points of the various components calculated for the same level of degradation coefficient (DC). The colour of each line represents the variation in the assumed level of degradation. The variation in the exergy destroyed was calculated as per Eq.(23). The exergy analysis enables identifying the contribution of the system components to the thermal efficiency penalties when the heat exchangers are degraded.

$$\text{Change in } \hat{\dot{E}x}_{dest} = \hat{\dot{E}x}_{dest,deg} - \hat{\dot{E}x}_{dest,DP} \tag{23}$$

The exergy analysis showed that the intercooler degradation (Fig. 5a) causes a change in the exergy destroyed within the Low Pressure Compressor (LPC), the saturator, the recuperator, the main combustion chamber and the reheater. ForDC_{IC} = 1, the exergy destroyed within the LPC increases by 0.12 pp, within the intercooler by

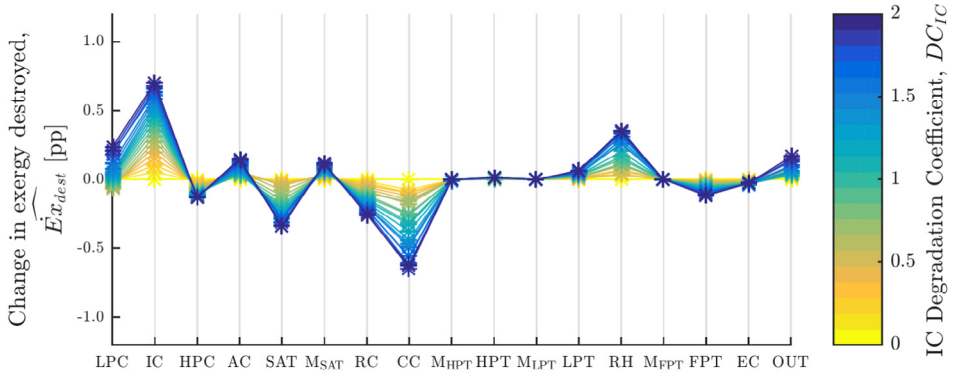

(a) Intercooler degradation.

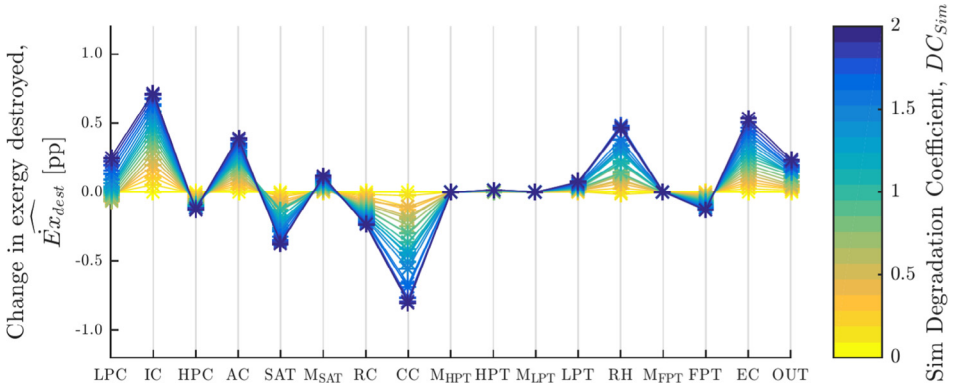

(b) Simultaneous heat exchanger degradation.

Fig. 5. Effect of the heat exchanger degradation on the exergy destroyed across the HAT system for the average effectiveness design scenario.

0.43 pp, and within the reheater by 0.15 pp. The exergy destroyed within the saturator reduced by 0.2 pp, within the recuperator by 0.15 pp, and within the combustion chamber by 0.26 pp. This implies that the LPC, intercooler, and reheater contribute towards the rise in the entropy generation, penalising the overall system's thermal efficiency. These effects are counter balanced by the exergy reductions occurring within the saturator, the recuperator, and the combustion chamber. Hence, the thermal efficiency penalty observed across the range of intercooler degradation levels, which can reach up to 0.7 pp for $DC_{IC} = 1$, is effectively the result of a trade-off between the performance improvements of the saturator, recuperator, and main combustion chamber, and the penalties caused by the LPC, intercooler and the reheater. The analysis also showed that the aftercooler and economiser deterioration cause no notable changes in the exergy distribution across the rest of system, where all air-water heat exchangers are degraded simultaneously (see Fig. 5b). Therefore, assuming that a change in the exergy destroyed is directly related with a change in the performance of the component, it can be seen that the deterioration of the intercooler causes a cascade effect that penalises the performance of several components across the entire system, whereas the degradation of the aftercooler and economiser only affects their own performance without notable knock on effects across the rest of the cycle. Fig. 6 shows the variation of the inlet mass flow, the specific power, the water to air ratio at the combustion chamber (ω_{CC}) and the recuperator effectiveness (ε_{RC}) when the air-water heat exchangers are degraded for the average heat exchanger effectiveness design scenario as the baseline configuration.

Fig. 6a shows that intercooler degradation causes the most detrimental effects in the overall mass flow through the system, an approximately 10% drop from the baseline value for$DC_{IC} = 1$. This reduction in mass flow triggers a small increase in the effectiveness of the recuperator (see Fig. 6b), which results in a higher gas temperature at the inlet of the main combustion chamber, reducing the required temperature rise across the burner. This yields the observed reduction in the relative exergy destroyed within the combustion chamber shown in Fig. 5. In the reheater, the temperature leap is kept constant since the free power turbine remains choked across the operating envelope, and the outlet is kept at 1600 K. However, the relative reduction in the exergy entering the cycle (lower temperature jump in the main combustion chamber) yields the increment of the relative exergy destroyed in the reheater for high levels of intercooler deterioration (see Fig. 5).

In terms of the saturator's operating condition, the increase in the injected water relative to the incoming air, caused the temperature leap between the water and the gas to reduce [50]. As a result, the heat and mass transfer process within the saturator tower becomes more efficient than at clean operation, which yields a decrease in exergy destruction across the saturator at degraded conditions (see Fig. 5). The rise in the injected water flow was derived from the increment of the air temperature at the entrance of the aftercooler, due to the degradation of the intercooling process, and at the entrance of the economiser, due to the lower pressure ratio (see Fig. 7). Therefore, because of the higher air inlet temperature, the water flow through these two heat exchangers was increased in order to avoid boiling.

In terms of the overall RHAT performance, the intercooler deteriorationcaused the high pressure compressor (HPC) inlet temperature to increase. This yielded higher required compressor work. At the same time an 8% reduction in the water to air ratio into the main combustion chamber was realised with regards to the clean operation (see Fig. 6c). The combination of these two effects, along with the mass flow reduction, caused the observed specific power output penalty of

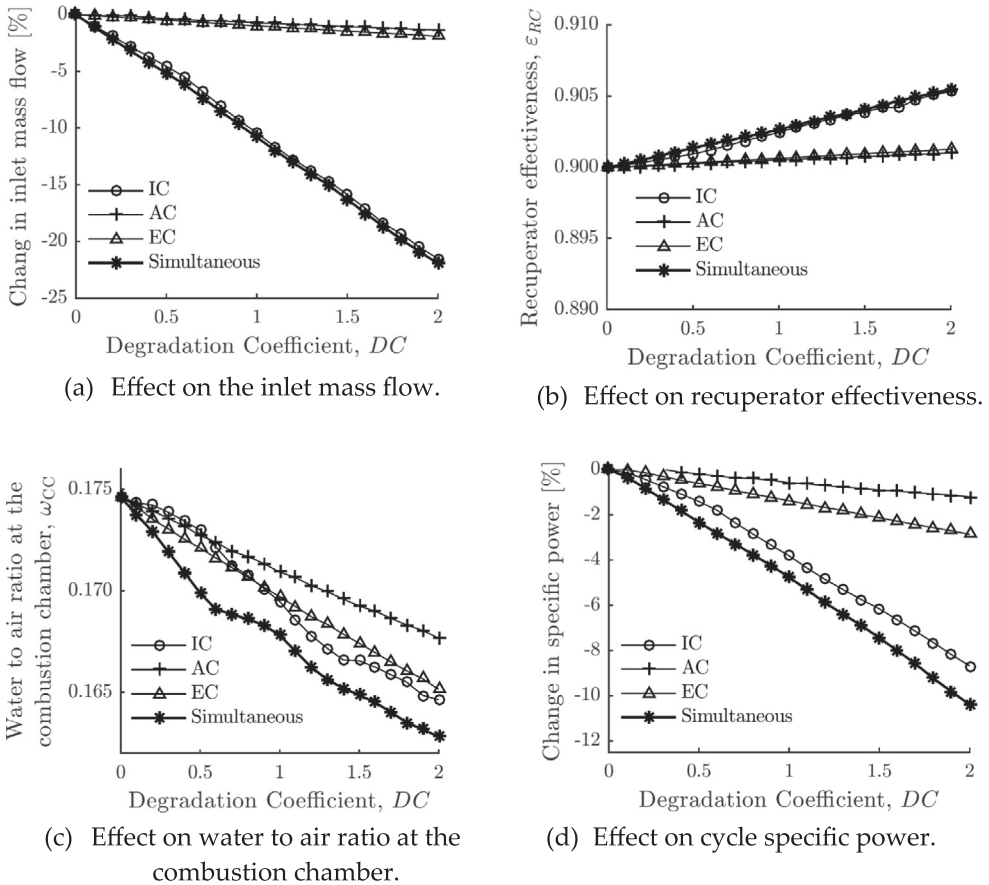

(a) Effect on the inlet mass flow.

(b) Effect on recuperator effectiveness.

(c) Effect on water to air ratio at the combustion chamber.

(d) Effect on cycle specific power.

Fig. 6. Effect of the heat exchanger degradation on the (a) inlet mass flow, (b) recuperator effectiveness, (c) water to air ratio and (d) specific power. Average heat exchanger effectiveness design scenario.

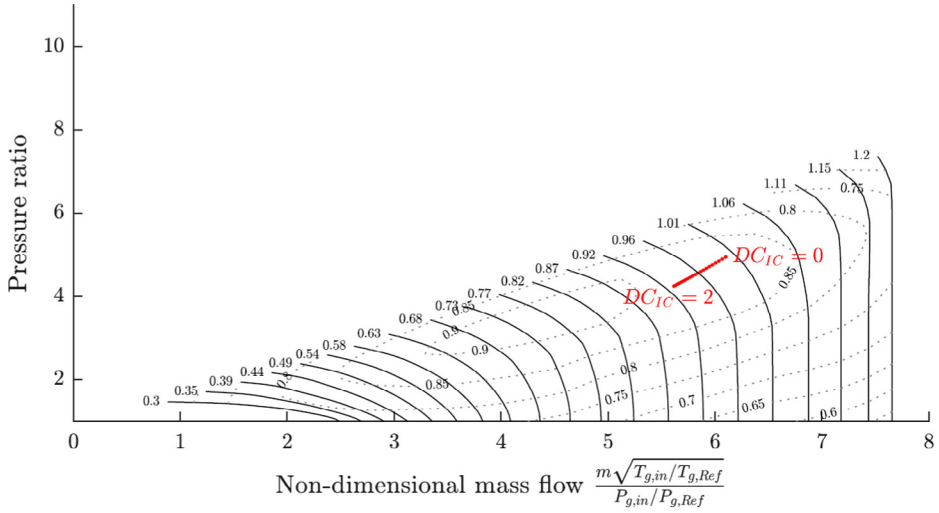

(a) High pressure compressor characteristic with running line.

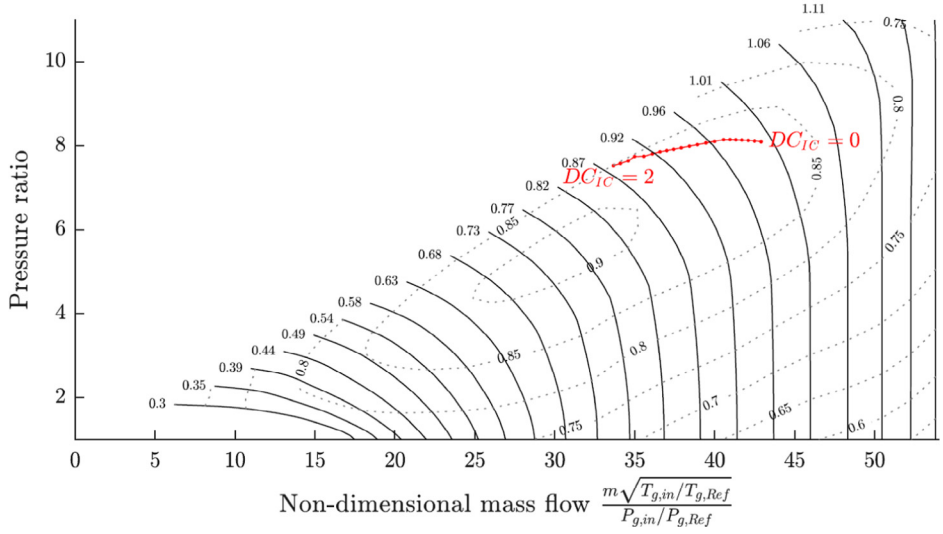

(b) Low pressure compressor characteristic with running line.

Fig. 7. Effect of intercooler's degradation on the compressor operating point for the average heat exchanger effectiveness design scenario. (a) High Pressure Compressor and (b) Low Pressure Compressor.

approximately 12% with reference to clean operation for $DC_{IC} = 2$ as shown in Fig. 6d. As expected, aftercooler and economiser degradation only weakly affect the penalties in the performance metrics of the RHAT system.

Finally, Fig. 7 shows the variation in the compressor operating points across a range of intercooler degradation levels for the average effectiveness design scenario as baseline. In the case of the High Pressure Compressor (HPC) (see Fig. 7a), the drop in non-dimensional flow and pressure ratio causes no notable penalty on the surge margin of the compressor. However, in the case of the LPC system (Fig. 7b), the reduction in the non-dimensional mass flow is more notable compared to the reduction in the pressure ratio for degraded operation of the air-water heat exchangers. This yields a considerable loss of surge margin as the intercooler deterioration levels increase which may result in unstable operation of the whole system. In addition, the shifting of the LPC's operating point to lower efficiency further justifies the increase in the exergy destroyed within this sub-system previously shown in Fig. 5.

4. Conclusions

The impact of air-water heat exchanger degradation on the performance of a reheated humid air turbine was herein analysed. Intercooler degradation was found to impose the most notable penalties on the thermal efficiency and the power output of the RHAT cycle, with a reduction up to 1.8 pp and 28% respectively for $DC_{IC} = 1$ and for an average nominal technology level of the heat exchangers. Aftercooler and economiser deterioration was found to have a weak impact on cycle performance. These performance penalties for $DC_{IC} = 1$ are also reflected in the mass flow through the system which drops by about 10% compared to the baseline as well as in the specific power output which shows an approximately 6% reduction form the nominal. The penalties in cycle performance become more significant as the baseline design effectiveness of all heat exchangers is reduced.

Exergy analysis enabled the identification of the main sources that cause changes in cycle performance when the heat exchangers are degraded. It is demonstrated that the degradation of the intercooler yields to notable performance penalties across the entire RHAT system, primarily at the low pressure compressor, the main combustion chamber and the reheater as the exergy destroyed within each of these parts increases when the intercooler deterioration coefficient varies between$DC_{IC} = 0$ and $DC_{IC} = 2$. On the other hand, performance enhancements were demonstrated at the saturator and the recuperator

units. The exergy analysis showed that the degradation of the economiser or the aftercooler does not affect the performance of the components across the rest of the system. In terms of the compressor operation, it is shown that intercooler degradation can cause loss of surge margin in the LPC, while the HPC system shows no operability penalties when the heat exchangers are degraded.

The outcomes of the present work indicate that from the system design point of view, heat exchangers of relatively high effectiveness are required especially in the case of the intercooler, as these show slower degradation rates. Nevertheless, the increased acquisition cost of a higher effectiveness intercooler should be taken into account at the economic assessment of the system and determine the exchange rate between the latter, thermal efficiency benefits, deterioration rate and maintenance cost. When it comes to the lower pressure compression system, a variable geometry configuration would potentially widen the operability range of the plant by mitigating the compressor surge risk at part-load operation. In addition, enhanced control of the LPC at part-load may also partially mitigate the efficiency penalties when the intercooler shows increased levels of degradation.

In general, this work has provided estimates of the performance penalties in terms of thermal efficiency and specific power output for a reheated humid air turbine system caused by the air-water heat exchanger's degradation. It has also identified the key parts of the system that are susceptible to these performance penalties which can further aid the design approach. Overall, this work has provided a step forward towards a better understanding of the RHAT cycle performance penalties associated with the degradation of the air-water heat exchanger units. This may be further used to aid the design and development of such power system for applications where high thermal efficiency is critical.

Acknowledgements

This research program is financially supported by an EPSRC Industrial CASE Award and Rolls-Royce plc. under the University Technology Centre in Aero System Design, Integration and Performance at Cranfield University. The authors kindly thank Rolls-Royce plc. for permission to publish this work. Due to confidentiality agreements with research collaborators, supporting data can only be made available upon reasonable request and with permission of the collaborator. Details of the data and how to request access are available at https://doi.org/10.17862/cranfield.rd.7527542.

References

[1] M. Jonsson, J. Yan, Humidified gas turbines—a review of proposed and implemented cycles, Energy 30 (7) (2005) 1013–1078, https://doi.org/10.1016/j.energy.2004.08.005.
[2] M. Yagi, H. Araki, H. Tagawa, T. Koganezawa, C. Myoren, T. Takeda, Progress of the 40 MW-class advanced humid air turbine tests, J. Eng. Gas Turbines Power 135 (11) (2013), https://doi.org/10.1115/1.4025037.
[3] A.D. Rao, Process for Producing Power, 1989.
[4] A. Lazzaretto, F. Segato, Thermodynamic optimization of the HAT cycle plant structure. Part I: Structure of the heat exchanger network, J. Eng. Gas Turbines Power 123 (January) (2001), https://doi.org/10.1115/1.1339000.
[5] A. Lazzaretto, F. Segato, Thermodynamic optimization of the HAT cycle plant structure. Part II: Structure of the heat exchanger network, J. Eng. Gas Turbines Power 123 (January) (2001), https://doi.org/10.1115/1.1339000.
[6] N.D. Ågren, M.O.J. Westermark, Design study of part-flow evaporative gas turbine cycles: performance and equipment sizing. Part II: Industrial core, J. Eng. Gas Turbines Power 125 (2003) 216–227, https://doi.org/10.1115/1.1476925.
[7] N.D. Ågren, M.O.J. Westermark, Design study of part-flow evaporative gas turbine cycles: performance and equipment sizing. Part I: Aeroderivative core, J. Eng. Gas Turbines Power 125 (2003) 201–215, https://doi.org/10.1115/1.1476924.
[8] P. Chiesa, G. Lozza, E. Macchi, S. Consonni, An assessment of the thermodynamic performance of mixed gas-steam cycles Part B- Water-injected and hat cycles, J. Eng. Gas Turbines Power 117 (3) (1995) 499–508, https://doi.org/10.1115/1.2814122.
[9] M. Nakhamkin, E.C. Swensen, J.R. Scheibel, A. Cohn, CHAT technology: an alternative approach to achieve advanced turbine systems efficiencies with present combustion turbine technology, in: ASME International Gas Turbine and Aeroengine Congress and Exhibition, Paper No. 98-GT-43, ASME, Stockholm, Sweden, Jun. 1998.
[10] G. Brighenti, P.L. Orts-Gonzalez, L. Sanchez, P.K. Zachos, Design point performance and optimization of humid air turbine power plants, Appl. Sci. 7 (4) (2017), https://doi.org/10.3390/app7040413.
[11] M. Jonsson, J. Yan, Economic assessment of evaporative gas turbine cycles with optimized part flow humidification systems, in: Proceedings of ASME Turbo Expo, Paper No. GT2003-38009, vol. 3, ASME, Atlanta, Georgia, USA, 2003.
[12] R.M. Kavanagh, G.T. Parks, A systematic comparison and multi-objective optimization of humid power cycles—Part I: thermodynamics, J. Eng. Gas Turbines Power 131 (2009), https://doi.org/10.1115/1.3026562.
[13] R.M. Kavanagh, G.T. Parks, A systematic comparison and multi-objective optimization of humid power cycles—Part II: Economics, J. Eng. Gas Turbines Power 131 (2009), https://doi.org/10.1115/1.3026562.
[14] A. Traverso, A.F. Massardo, Thermoeconomic analysis of mixed gas-steam cycles, Appl. Therm. Eng. 22 (1) (2002), https://doi.org/10.1016/S1359-4311(01)00064-3.
[15] T. Takahashi, Y. Nakao, E. Koda, Analysis and evaluation about advanced humid air turbine system, Challenges of Power Engineering and Environment, Springer Berlin Heidelberg, Berlin, Heidelberg, 2007, pp. 341–344.
[16] B. Wang, S. Zhang, Y. Xiao, Steady state off-design performance of humid air turbine cycle, in: Proceedings of ASME Turbo Expo, Paper No. GT2007-27350, ASME, Montreal, Canada, 2007, pp. 139–149.
[17] T.S. Kim, C.H. Song, S.T. Ro, S.K. Kauh, Influence of ambient condition on thermodynamic performance of the humid air turbine cycle, Energy 25 (4) (2000) 313–324, https://doi.org/10.1016/S0360-5442(99)00074-2.
[18] S. Kakaç, A. Pramuanjaroenkij, Heat Exchangers: Selection, Rating, and Thermal Design, CRC Press, Boca Raton, Florida, USA, 2012.
[19] V. Gesellschaft, VDI Heat Atlas, second ed., Springer Science & Business Media, Berlin, Germany, 2010.
[20] W.J. Marner, J.W. Suitor, A Survey of Gas-Side Fouling in Industrial Heat-Transfer Equipment, NASA Report, 1983.
[21] H. Barrow, K. Sherwin, Theoretical investigation of the effect of fouling on the performance of a tube and plate fin heat exchanger, Heat Recovery Syst. CHP 14 (1) (1994) pp, https://doi.org/10.1016/0890-4332(94)90066-3.
[22] A. Zwebek, P. Pilidis, Degradation effects on combined cycle power plant performance—Part II: Steam turbine cycle component degradation effects, Journal of Engineering for Gas Turbines and Power 125 (3) (2003) 658, https://doi.org/10.1115/1.1519272.
[23] A. Zwebek, P. Pilidis, Degradation effects on combined cycle power plant performance—Part III: Gas and steam turbine component degradation effects, Journal of Engineering for Gas Turbines and Power 126 (2) (2004) 306–315, https://doi.org/10.1115/1.1639007.
[24] B. Nyberg, M. Thern, Thermodynamic studies of a HAT cycle and its components, Appl. Energy 89 (1) (2012) 315–321, https://doi.org/10.1016/j.apenergy.2011.07.036.
[25] M. Rosen, Evaporative Cycles - in Theory and in Practise, PhD Thesis Lund Institute of Technology, Lund, Sweden, 2000.
[26] R.C. Sanders, G.C. Louie, Development of the WR-21 Gas Turbine Recuperator, International Gas Turbine and Aeroengine Congress and Exhibition, Paper No. 99-GT-314, ASME, Indianapolis, Indiana, USA, Jun. 1999.
[27] G. Xiao, T. Yang, H. Liu, D. Ni, M.L. Ferrari, M. Li, Z. Luo, K. Cen, M. Ni, Recuperators for micro gas turbines: a review, Appl. Energy 197 (2017) 83–99, https://doi.org/10.1016/j.apenergy.2017.03.095.
[28] TEMA, Standards of the Tubular Exchanger Manufacturers Association, eighth ed., Technical Committee of the Tubular Exchanger Manufacturers Association, New York, USA, 1999.
[29] T.R. Bott, C.R. Bemrose, Particulate fouling on the gas- side of finned tube heat exchangers, J. Heat Transfer 105 (February) (1983) 178–183, https://doi.org/10.1115/1.3245538.
[30] B.C. Pak, J.B. Braun, E.A. Groll, Impacts of fouling and cleaning on the performance of plate fin and spine fin heat exchangers, KSME Int. J. 17 (11) (2003) 1801–1811, https://doi.org/10.1007/BF02983611.
[31] G.D. Brighenti, P.K. Zachos, P.L. Orts-Gonzalez, Part-load performance modelling of a reheated humid air turbine power cycle, Appl. Therm. Eng. 138 (April) (2018) 365–373, https://doi.org/10.1016/j.applthermaleng.2018.04.056.
[32] W.L. Macmillan, Development of a Module Type Computer Program for the Calculation of Gas Turbine Off Design Performance, PhD Thesis Cranfield University, Cranfield, UK, 1974.
[33] A. Pellegrini, T. Nikolaidis, V. Pachidis, S. Köhler, On the performance simulation of inter-stage turbine teheat, Appl. Therm. Eng. 113 (2017) 544–553, https://doi.org/10.1016/j.applthermaleng.2016.10.034.
[34] A. Aramayo-Prudencio, J.B. Young, The analysis and design of saturators for power generation cycles: Part 2 - Heat and mass transfer, Proceedings of ASME Turbo Expo, Paper No. GT2003-38946, ASME, Atlanta, Georgia, USA, 2003, pp. 423–432.
[35] T. Lindquist, M. Thern, T. Torisson, Experimental and theoretical results of a humidification tower in an evaporative gas turbine cycle pilot, Plant Proceedings of ASME Turbo Expo, Paper No. GT2002-30127, ASME, Amsterdam, Netherlands, 2002, pp. 475–484.
[36] C.G. Broyden, A class of methods for solving nonlinear simultaneous equations, Math. Comput. 19 (92) (Oct. 1965) 577–593, https://doi.org/10.2307/2003941.
[37] ESDU, High-Fin Staggered Tube Banks: Heat Transfer and Pressure Drop for Turbulent Single Phase Gas Flow, ESDU Data Items, No. Data Item No. 86022, 1988.
[38] W.M. Kays, A.L. London, Compact heat exchangers, third ed., Krieger Pub. Co, New York, USA, 1984.
[39] P.P. Walsh, P. Fletcher, Gas turbine performance, second ed., Blackwell Science Ltd, Oxford, UK, 2004.

[40] ESDU, Forced Convection Heat Transfer in Straight tubes. Part 1: Turbulent Flow, ESDU Data Items, No. Data Item No. 92003, 1993.
[41] C. Ezgi, N. Özbalta, I. Girgin, Thermohydraulic and thermoeconomic performance of a marine heat exchanger on a naval surface ship, Appl. Therm. Eng. 64 (1–2) (2014) 413–421, https://doi.org/10.1016/j.applthermaleng.2013.12.061.
[42] Y. Söhret, S. Ekici, Ö. Altuntaş, A. Hepbasli, T.H. Karakoç, Exergy as a useful tool for the performance assessment of aircraft gas turbine engines: A key review, Progr. Aerosp. Sci. 83 (May) (2016) 57–69, https://doi.org/10.1016/j.paerosci.2016.03.001.
[43] M. Jonsson, J. Yan, Exergy analysis of part flow evaporative gas turbine cycles: Part 2 — Results and discussion, Proceedings of ASME Turbo Expo, Paper No. GT2002-30126, ASME, Amsterdam, Netherlands, 2002, pp. 465–473.
[44] A. Kumari, Sanjay, Investigation of parameters affecting exergy and emission performance of basic and intercooled gas turbine cycles, Energy 90 (2015) 525–536, https://doi.org/10.1016/j.energy.2015.07.084.
[45] M.Z. Sogut, E. Yalcin, T.H. Karakoc, Assessment of degradation effects for an aircraft engine considering exergy analysis, Energy (2017), https://doi.org/10.1016/j.energy.2017.03.093.
[46] C.T. Yucer, Thermodynamic analysis of the part load performance for a small scale gas turbine jet engine by using exergy analysis method, Energy 111 (2016) 251–259, https://doi.org/10.1016/j.energy.2016.05.108.
[47] Y.A. Çengel, M.A. Boles, Thermodunamics: An Engineering Approach, fifth ed., McGraw-Hill, Boston, MA, USA, 2006.
[48] F. Dalili, M. Andrén, J. Yan, M. Westermark, The impact of thermodynamic properties of air-water vapor mixtures on design of evaporative gas turbine cycles, in: Proceedings of ASME Turbo Expo, ASME, New Orleans, Lousiana, USA, 2001.
[49] A.W. Date, Analytic Combustion: With Thermodynamics, Chemical Kinetics and Mass Transfer, Cambridge University Press, Cambridge, UK, 2011.
[50] A. Aramayo-Prudencio, J.B. Young, The analysis and design of saturators for power generation cycles: Part 1 - Thermodynamics, in: Proceedings of ASME Turbo Expo, Paper No. GT2003-38945, ASME, Atlanta, Georgia, USA, 2003, pp. 411–421.